Light, Small Angle Neutron and X-Ray Scattering from Gels

Erik Geissler,[*1] *Anne-Marie Hecht,*[1] *Cyrille Rochas,*[1] *Ferenc Horkay,*[2] *Peter J. Basser*[2]

[1]Laboratoire de Spectrométrie Physique CNRS UMR 5588, Université J. Fourier de Grenoble, B.P. 87, 38402 St Martin d'Hères cedex, France
[2]Section on Tissue Biophysics and Biomimetics, Laboratory of Integrative and Medical Biophysics, NICHD, National Institutes of Health, 13 South Drive, Bethesda, MD 20892, USA

Summary: This paper gives two examples of experiments that demonstrate the power of small angle scattering techniques in the study of swollen polymer networks. First, it is shown how the partly ergodic character of these systems is directly detected by neutron spin echo experiments. The observed total field correlation function of the intensity scattered from a neutral gel allows the ergodic contribution to be directly distinguished from the non ergodic part, at values of transfer wave vector q that lie well beyond the range of dynamic light scattering. The results can be compared with those obtained at much lower q from visible light scattering.
Second, a recent application of small angle X-ray (SAXS) and neutron (SANS) scattering is described for a polyelectrolyte molecule, DNA, in semi-dilute solutions under near-physiological conditions. For these observations, the divalent ion normally present, calcium, is replaced by an equivalent ion, strontium. The comparison between SANS and SAXS yields a quantitative picture of the cloud of divalent counter-ions around the central DNA core. At physiological conditions, the cloud is thinner than that predicted on the basis of the Debye screening length but thicker than if the counter-ions were condensed on the DNA chain.

Keywords: counter-ion cloud; DNA; dynamic light scattering; neutralized polymer gels; polymer gels; small angle neutron scattering

Introduction

The scattering of photons or neutrons by polymer gels and solutions yields information not only on the structure and distribution of the different components in the system, but also on their dynamics. Chemically cross-linked polymer gels are interesting in that at short (nanometre) distance scales they behave like liquids, while on a larger (> 100 nanometre) scale they are elastic solids. In such soft gels the network chains are mobile. Thermally driven conformation changes of the network chains not only govern the diffusion of the solvent molecules in the network by perpetually mingling both components but also exert an osmotic pressure that causes the gel to swell. Not all gel systems, however, display liquid-like properties at short distance scales: many physical gels are composed of rod-like polymers

with few degrees of freedom and exhibiting reduced osmotic pressure (in polyelectrolytes, however, a major contribution to the osmotic pressure stems from the counter-ions). Such structures are predominantly static. This article addresses gels of both kinds, the first by using neutron spin echo (NSE), dynamic light scattering (DLS) and small angle neutron scattering (SANS). Small angle X-ray scattering (SAXS) is also reported in a system of the second kind, namely concentrated solutions of DNA, in order to determine the structure of the counter-ion cloud surrounding the polymer backbone.

Experimental Section

Dynamic light scattering measurements were performed on an ALV compact goniometer equipped with a 22 mW HeNe laser working at 6328 Å. The NSE measurements were made on the IN15 instrument at the Institut Laue-Langevin, Grenoble with an incident wavelength of 15 Å. The SAXS measurements were done at beam line BM2 at the European Synchrotron Radiation Facility, Grenoble, with an incident energy that was varied between 14.8 keV and 16.102 keV, the latter being close to the absorption edge of strontium. SANS measurements were made on the NG3 30m instrument at NIST, Gaithersburg, using as solvent a $92\%H_2O\,8\%D_2O$ mixture to eliminate hydration effects. The wave vector is $q = |\mathbf{q}| = (4\pi n/\lambda)\sin(\theta/2)$, where θ is the scattering angle, n the refractive index of the medium and λ the wavelength of the incident radiation.

Results and Discussion

SANS, NSE and DLS in gels of the first kind

Light scattering and SANS yield similar information on the structure of polymer systems, but, owing to the difference in wavelength of the two types of radiation, they generally probe complementary q-ranges. Integrated light scattering, like SANS, detects not only the static structures in a gel but also the liquid-like parts. NSE, on the other hand, like DLS, discriminates between the dynamic and the static components that are present in polymer gels. The first of these techniques, by varying the magnetic field in the neutron flight path, measures directly the field correlation function $g(t)$ of the scattered neutrons, while the second detects the intensity correlation function $G(t)$ of the scattered light. It is frequently found that the total scattering spectrum of a gel can be expressed in the form

$$I(q) = I_{\text{stat}}(q) + I_{\text{dyn}}(q) \tag{1}$$

in which the first term describes the solid-like and the second the liquid-like properties. The fluctuating nature of the second term can be detected by both DLS and NSE. Fig. 1 shows the

decay of the neutron echo amplitude as a function of time in a fluorinated silicone gel, swollen in acetone.[1] To enhance the contrast between polymer and solvent the acetone was deuterated.
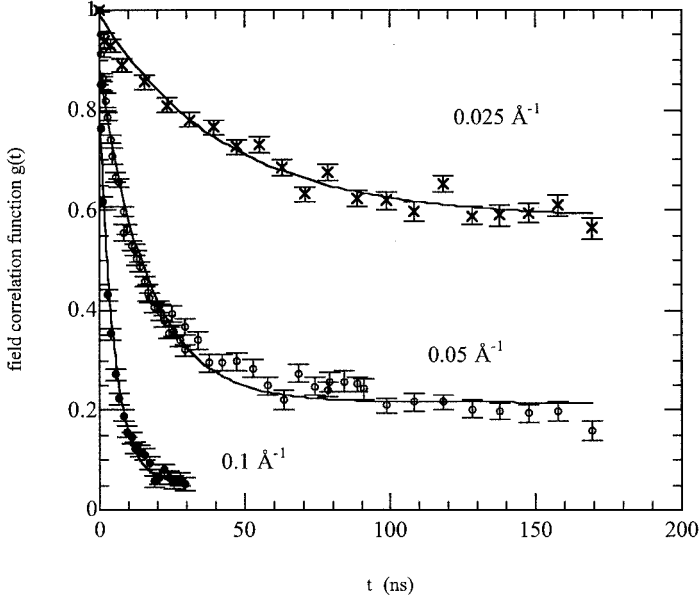

Figure 1. Spin echo amplitude $g(t)$ as a function of delay time t in a fluorinated silicone gel swollen in deuterated acetone. Continuous curves are fits to eq. 2 for the different values of q indicated. Note the time scale in nanoseconds.

It is found that in each case the normalised NSE decays can be described by the expression

$$g(t) = a_0(q) + a_1(q) \exp(-\Gamma t) \tag{2}$$

in which the first term is the static component and the second is the fluctuating part. In uncross-linked solutions, $a_0(q) = 0$, since there are no static structures. From eq. 1 we may write

$$I_{stat}(q) = a_0(q)\, I(q) \text{ and } I_{dyn}(q) = a_1(q)\, I(q) \tag{3}$$

while the relaxation rate Γ of the fluctuations is governed by the collective diffusion in the gel

$$\Gamma = Dq^2 \tag{4}$$

Satisfactory fits of the SANS data to eq 1 are found by assuming a Debye-Bueche form[2] for the static scattering and an Ornstein-Zernicke form for the dynamic. Thus

$$I_{stat}(q) = \Delta\rho^2 8\pi\Xi^3 \delta\varphi^2/(1+q^2\Xi^2)^2 \text{ and } I_{dyn}(q) = \Delta\rho^2 (kT\varphi^2/M_{os})/(1+q^2\xi^2) \tag{5}$$

in which $\Delta\rho^2$ is the neutron scattering contrast, φ is the polymer volume fraction, $\delta\varphi^2$ the

mean square amplitude of the static concentration fluctuations due to cross-links and Ξ the correlation length of the static heterogeneities.[3] M_{os} is the osmotic modulus of the gel and ξ the correlation length of the dynamic concentration fluctuations. Fitting eq. 5 to the data, shown in Figure 2, involves 4 adjustable parameters, namely two amplitudes and two correlation lengths.
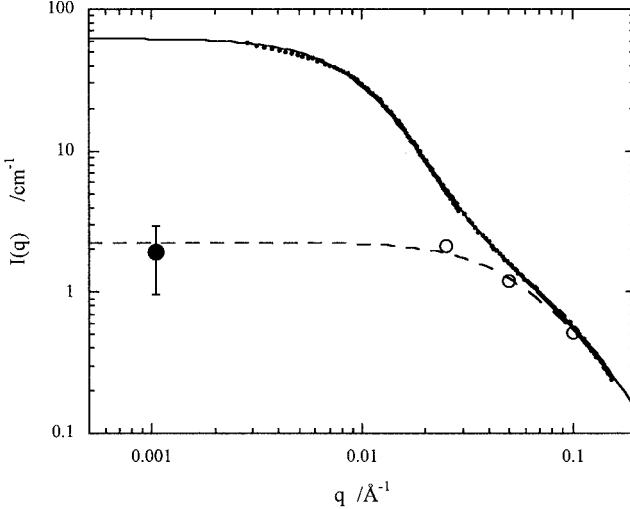

Figure 2. Total SANS intensity $I(q)$ with fit to eq 5 (continuous curve, Ξ = 71 Å, ξ = 20 Å). Dashed curve: $I_{dyn}(q)$ from this fit. Open circles: amplitude $I_{dyn}(q)$ from NSE and eq 3; filled symbol: $I_{dyn}(q)$ from DLS.[1]

The above results may be compared with those of dynamic light scattering. Unlike neutrons, whose spatial wave functions are incoherent, laser light has a high degree of coherence, which generates optical heterodyning between the dynamically light scattered and that scattered elastically from the static structure. The requisite field correlation function $g(t)$ must be determined from the quantity measured by DLS, namely the intensity correlation function $G(t)$, where[4,5]

$$G(t) = 1 + \beta[2X(1-X)g(t) + X^2g(t)^2], \quad X = I_{dyn}(q)/I(q) \tag{6}$$

where β is the optical coherence factor of the apparatus. Figure 3 shows an example of this procedure for a similar gel (poly N-isopropyl acrylamide/water at 20°C).[6] Measurements of the intensity were made at a fixed scattering angle (90°) for various sample positions. This brings bright or dark static speckles into the view of the detector, each position giving a different value of X, and each time a new correlation function is accumulated. As can be seen

in the figure the dynamic intensity $I_{dyn}(q)$ and the field correlation function are, within experimental error, both independent of X.
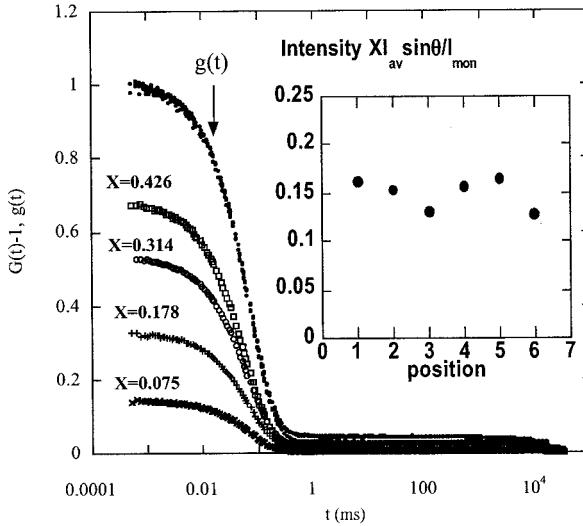

Figure 3. DLS measurements of the intensity correlation function $G(t)$ for various sample positions with different speckle intensities, defined by $X=I_{dyn}(q)/I(q)$ at the same scattering angle. The field correlation function $g(t)$ (upper curve) and the dynamic intensity (inset) are both independent of the static speckle intensity.[5]

Returning now to Figure 2, the filled symbol indicates the value of $I_{dyn}(q)$ obtained in this way, after correction for the ratio of the corresponding contrast factors $\Delta\rho^2$ for neutrons and light. The agreement between the DLS and NSE results confirms the validity of eq. 1 according to which the scattering signal is separated into a dynamic and a static contribution. Since $I_{dyn}(q)$ is independent of the static speckle pattern, it can be concluded that the movement of the network chains is *ergodic*, i.e., they are effectively delocalized. The larger scale elastic inhomogeneities, on the other hand, are strongly localized and are thus non-ergodic,[7] producing the plateau $a_0(q)$ in the NSE decays of Fig. 1.

SAXS in gels of the second kind

In semi-dilute solution, high molecular weight polyelectrolytes possess viscoelastic properties that correspond to gels with temporary cross-links. The long range Coulomb repulsion in highly charged polymers favours an extended conformation that, for DNA, would cause it to exceed the size of a biological cell. In its biological functions, however, the DNA morphology is governed by the counter-ion environment, which can modify the electrostatic interactions at several distance scales. A knowledge of the counter-ion distribution is

therefore essential for the understanding of the biological function of this molecule. In particular, the effect of multivalent ions on the chain conformation is poorly understood.

Simulations based on molecular dynamics modelling have shown that in the presence of divalent counter-ions, short range attractive interactions generate aggregation of the DNA strands, resulting in the formation of bundles and other partially ordered arrangements.[8,9] Present molecular dynamics approaches do not, however, explicitly address the localization of multivalent cations along the backbone of the polymer.

Here small angle X-ray scattering (SAXS) and small angle neutron scattering (SANS) are combined to determine the distribution of small divalent counter-ions around high molecular mass DNA (DNA sodium salt, salmon testes, Sigma) under physiological conditions, i.e., where monovalent counter-ions are also present. Strontium, which mimics the physiological divalent ion, calcium, is also investigated. In DNA solutions of high molecular mass, increasing the concentration of alkali earth metal ions such as calcium or strontium leads to replacement of the sodium counter-ions and ultimately causes reversible phase separation. In principle, varying the wavelength of the incident beam in the vicinity of the absorption edge of the counter-ion (anomalous SAXS, or ASAXS) yields information simultaneously on the distribution of ions and on the polymer.[10-14] In practice, however, the relative variation in electronic contrast explored in an ASAXS measurement on an electron rich molecule such as DNA is small, thus making it difficult to draw conclusions. The differences between neutron and X-ray scattering contrast small angle neutron scattering (SANS) measurements provide valuable complementary information on the structural contributions of the polymer and of the surrounding ions.[15-18] At high values of the transfer wave vector q, however, where scattering techniques are sensitive to the local structure of the polymer and the counter-ion distribution, the signal to noise ratio in SANS experiments becomes poor. For this reason it is desirable to combine observations both of SAXS and SANS.

Figure 4 shows the SANS spectra of two DNA solutions in 100 mM NaCl. In the presence of calcium chloride, such solutions act as ion exchangers and concentrate the calcium ions from the surrounding environment. To mimic this effect, 80 mM of calcium chloride and strontium chloride was added to the solutions, a quantity below that required to cause phase separation (ca.100 mM). Within experimental error the SANS response in the presence of these two ions is identical.[19]

Figure 5 shows a Kratky plot of the signal obtained by SAXS from two calcium containing samples. The characteristic oscillatory scattering function from a cylinder is clearly revealed.
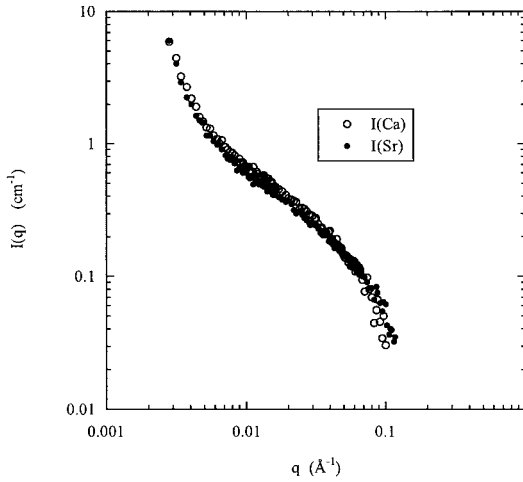
Figure 4. SANS response from a 3 wt% DNA solution containing 100 mM NaCl and 80 mM CaCl$_2$ (open symbols) or 80 mM SrCl$_2$ (filled symbols) in a 8%D$_2$O - 92% H$_2$O mixture.[18]
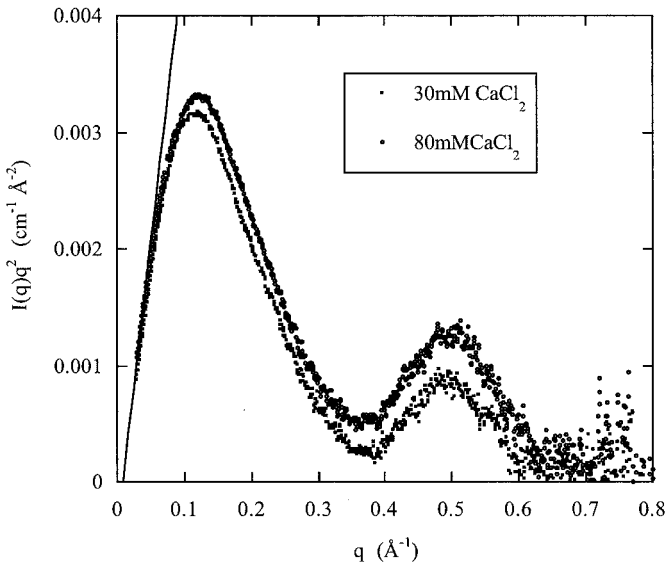

Figure 5. Kratky plot of 3 %wt solutions of DNA containing 30 mM and 80 mM CaCl$_2$ (open symbols). The asymptotic straight line at the left of the figure yields the mass per unit length and the apparent persistence length L of the rod-like DNA in solution.

To describe the SAXS signal, the following semi-empirical expression,[20] analogous to expression 5, is used

$$I(q) = K^2 r_0^2 \left\{ \frac{kT\varphi^2}{M_{os}(1+qL)} \left[\frac{2J_1(qr)}{qr} \right]^2 + aq^{-m} \right\} \tag{7}$$

where K is the electron density between the DNA molecule and the surrounding solution, r_0 the classical radius of the electron, L is the effective persistence length of the polymer in the solution of overlapping DNA molecules, $J_1(x)$ is the Bessel function of order one and the exponent m in the power law term describes the scattering at low q from large-scale heterogeneities in the DNA solution. Equation 7, which has been found to describe the scattering from solutions containing rod-like elements such as polyelectrolytes, assumes that the divalent counter-ion cloud surrounding the DNA molecule has the same shape, i.e., it is condensed on the molecule, as may be expected in an ion exchange situation.
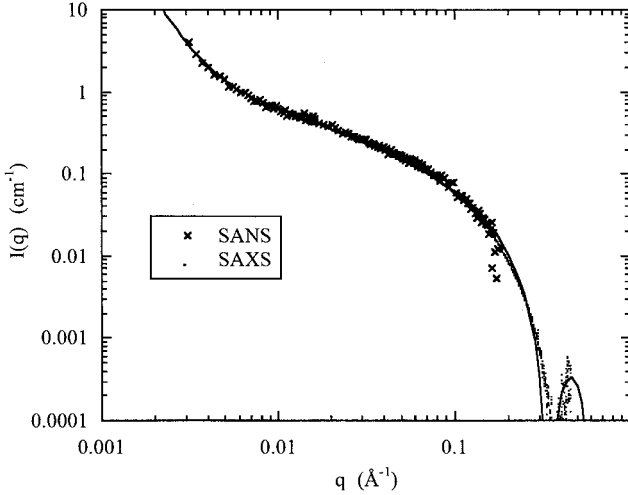

Figure 6. SANS (×) and SAXS (•)scattering intensity from a 3 wt% DNA solution containing 100 mM NaCl and 80 mM SrCl$_2$. Continuous curve is the least squares fit to eq 7.

Although the result of the fit of eq 7, shown in Figure 6, accounts for the main features of the scattering, with $L=200$Å and $r=11.1$ Å, the value found for the radius of the DNA molecule r is larger than that indicated by the position of the two minima in Figure 5 (10.0Å). A different model for the counter-ion distribution is therefore adopted, illustrated in Fig. 7. In this model the total charge of the counter-ion cloud is taken to be uniformly distributed in an annular space of outer diameter r_2 surrounding the molecule. The model, which guarantees the overall electrical neutrality of the DNA molecule, allows the ratio $p=r_2/r_1$ to be varied, while taking into account variations in excess electron density due to dilution of the strontium ions in the
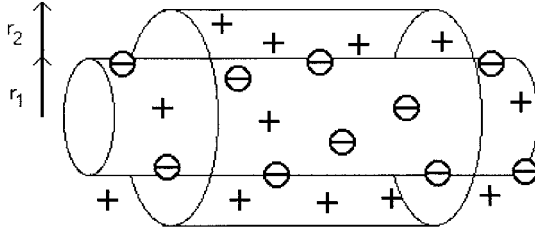
Figure 7. Model used in this study. DNA core of radius r_1 decorated on its surface with negatively charged groups ($\ominus$), enclosed by sheath of outer radius r_2 containing the mobile counter-ions ($+$).

cylindrical sheath. The resulting expression for the SAXS scattering intensity then becomes

$$I(q) = \frac{kT\varphi^2 r_0^2}{M_{os}(1+qL)} \left\{ \left(K_p - \frac{Z_{tot}}{\pi r_1^2 b\left(p^2 - 1\right)} \right) \frac{2J_1(qr_1)}{qr_1} + p^2 \left[\frac{Z_{tot}}{\pi r_1^2 b\left(p^2 - 1\right)} \frac{2J_1(pqr_1)}{pqr_1} \right] \right\}^2 \tag{8}$$

where K_p the difference in electron density the between the DNA core and the solvent, Z_{tot} the effective electron density of the strontium ion and its hydration sphere and b is the base pair spacing in DNA. This approach, in which r_1 and p are varied to yield a fit to the experimental data, does not rely on the Poisson-Boltzmann equation to define the spatial extent of the counter-ion cloud.
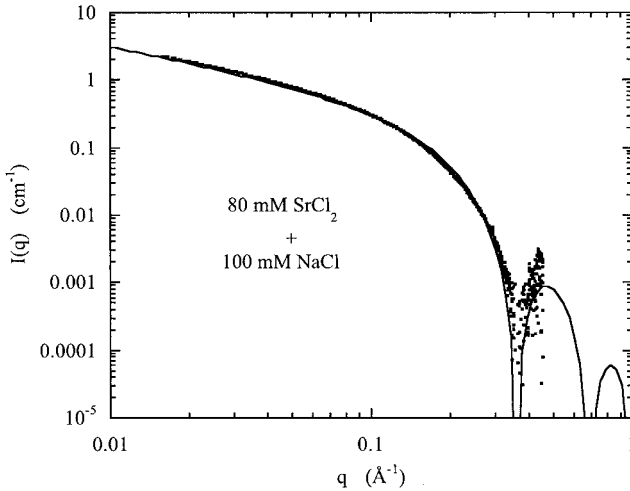

Figure 8. Fit of eq 8 to SAXS data from a 3 %wt DNA solution containing 100 mM NaCl and 80 mM SrCl$_2$.

Figure 8 shows the result of fitting eq 8 to the solution containing 80 mM $SrCl_2$. In each case, the agreement with the data is notably improved over eq 7. This finding indicates that the counter-ion cloud is not condensed on the surface of the DNA molecule, but is confined to a narrow region outside. The thickness of this annular space, $(p-1)r_1$, should be compared with the Debye screening length Λ_D. In the present cylindrical geometry, however, a more appropriate comparison is with Δ_D, which describes the increase in mean square radius of the ion cloud around a uniformly charged cylinder. Thus

$$r_2^2 = \left(r_1 + \Delta_D\right)^2 = \int_{r_1}^{\infty} 2\pi r^3 \exp(-r/\Lambda_D)dr / \int_{r_1}^{\infty} 2\pi r \exp(-r/\Lambda_D)dr \qquad (9)$$

In Table I it can be seen that in each case the thickness of the counter-ion cloud, $(p-1)r_1$, is less than Δ_D. The present results thus show that the divalent counter-ions around the DNA strand are not physically adsorbed on the surface of the molecule but are confined to a sheath of effective thickness smaller than the Debye screening length.

Table 1. Comparison of thickness of counter-ion sheath with effective Debye screening distance.

Sample	Counter-ion sheath thickness $(p-1)r_1$ (Å)	Debye screening length Λ_D (Å)	Effective Debye screening distance Δ_D (Å)
DNA $SrCl_2$ 30 mM	3.8	5.0.	7.8
DNA $SrCl_2$ 80 mM	3.8	3.9	5.4
DNA $CaCl_2$ 30 mM	5.5	5.0	7.8
DNA $CaCl_2$ 80 mM	3.8	3.9	5.4

[1] A.-M. Hecht, F. Horkay, P. Schleger, E. Geissler, *Macromolecules* **2002**, *35*, 8552.

[2] P. Debye, R.M. Bueche, *J. Appl. Phys.* **1949**, *20*, 518.

[3] E. Geissler, F. Horkay, A.-M. Hecht, *Phys. Rev. Lett.* **1993**, *71*, 645.

[4] E. Geissler in *Dynamic Light Scattering* Ed. W. Brown, Oxford 1993.

[5] F. Horkay, W. Burchard, E. Geissler, A.M. Hecht *Macromolecules* **1993**, *26*, 1296.

[6] K. László, K. Kosik, C. Rochas, E. Geissler *Macromolecules* **2003**, *36*, 7771.

[7] P.N. Pusey, W van Megen *Physica A* **1989**, *157*, 705.

[8] M.J. Stevens, *Phys. Rev. Lett.* **1999**, *82*: 101.

[9] M.J. Stevens, *Biophys. J.* **2001**, *80*, 130.

[10] C.E. Williams, In *Neutron, X-ray and Light Scattering*. Eds. P. Lindner, T. Zemb. Elsevier BV 1991.

[11] I. Sabbagh, M. Delsanti, P. Lesieur, *Eur. Phys. J. B* **1999**, *12*, 253.

[12] B. Guilleaume, J. Blaul, M. Ballauff, M. Wittemann, M. Rehahn, G. Goerigk, *Eur. Phys. J. E* **2002**, *8*, 299.

[13] G. Goerigk, R. Schweins, K. Huber, M. Ballauff, *Europhys. Lett.* **2004**, *66*, 331.

[14] R. Das, T.T. Mills, L.W. Kwok, G.S. Maskel, I.S. Millet, S. Doniach, K.D. Finkelstein, D. Herschlag, L. Pollack,. *Phys. Rev. Lett.* **2003**, 90, 188103.

[15] J.R.C. van der Maarel, L.C.A. Groot, M. Mandel, W. Jesse, G. Jannink, V. Rodriguez, *J. Phys. II France* **1992**, *2*, 109-122.

[16] J.R.C. van der Maarel, K. Kassapidou, *Macromolecules* **1998**, *31*, 5734.

[17] S.S. Zakharova, S.U. Egelhaaf, L.B. Bhuiyan, C.W. Outhwaite, D. Bratko, J.R.C. van der Maarel, *J. Chem. Phys.* **1999**, *111*, 10706.

[18] I.Morfin, F. Horkay, P.J. Basser, F. Bley, F. Ehrburger-Dolle, A.-M. Hecht, C. Rochas, E. Geissler, *Macromolecular Symposia* **2003**, *200*, 227.

[19] I.Morfin, F.Horkay, P.J.Basser, F. Bley, A.-M.Hecht, C. Rochas, E. Geissler, *Biophys. J.* **2004**, *87*, 2897.

[20] F. Horkay, A.-M. Hecht, I. Grillo, P.J. Basser, E. Geissler, *J. Chem. Phys.*, **2002**, *117*, 9103.